Volume 14-Issue 2 (2025)

Journal of Transportation Science and Technology

Journal homepage: https://tapchicongnghegtvt.vn

A Study on Numerical Simulation to Analyze the Behavior of Reinforced Concrete Technical Manholes

SyDan Dao*
Faculty of Civil Engineering, University of Transport and Communications

Keywords:
Numerical simulation
Highways
Technical manholes
Reinforced concrete
Plaxis

ABSTRACT

With the rapid development of infrastructure, technical manholes play a crucial role in the construction of drainage systems and utility conduits. This paper presents a numerical simulation method for analyzing the behavior of reinforced concrete technical manholes on highways in Vietnam using Plaxis 3D software. The study focuses on large, cast-in-place technical manholes, which are subjected to complex loading conditions, including surrounding soil pressure, water pressure, and live loads from vehicles. The results demonstrate that the primary internal force components (bending moments and shear forces) can be accurately determined, providing a foundation for verifying or designing reinforced concrete manholes in highway projects in Vietnam. The results for bending moments and shear forces calculated using the approximate method are overly conservative; they are about 1.4 times greater than the results obtained from the numerical method. This method offers valuable insights for optimizing the design process, reducing material costs, and providing a more precise approach compared to traditional manual calculations. The findings contribute to improving the design and construction of reinforced concrete technical manholes in Vietnam's highway infrastructure.

1. Introduction

Nowadays, along with the rapid development of the economy, the infrastructure systems in new urban areas and highways are increasingly being constructed in Vietnam to meet the growing demands for living, transportation, and goods delivery. Along with these, technical manholes are being constructed in a coordinated manner to accommodate drainage pipes and utility conduits. For small technical manholes, we can use precast reinforced concrete manholes, designed according to TCVN 10333 – Precast Thin Wall Reinforced Concrete Manholes [1]. For large urban areas or highways, technical manholes can sometimes have relatively large dimensions. In these cases, they are usually constructed using cast-in-place reinforced concrete to meet the specific size and strength requirements. In such cases, the technical manholes must be individually designed and calculated for each specific situation.

Reinforced concrete technical manholes are a complex type of structure, consisting of

* SyDan Dao. Faculty of Civil Engineering, University of Transport and Communications.
Email: sydandao@utc.edu.vn

https://www.doi.org/10.55228/JTST.14(2)142-150
Recieved: December 21, 2024; Recieved in revised: March 13, 2025; Accepted: March 14, 2025
Available online: March 15, 2025
pISSN: 1859-4263; eISSN: 3030-4261

multiple interconnected flat panels, statically indeterminate, and subjected to various complex loads, including the surrounding soil pressure, water in the soil, and live loads from above, such as human loads, equipment, and vehicular loads on top. In the past, before the availability of calculation software, the analysis of the behavior of technical manholes was typically done manually, requiring the acceptance of certain assumptions to simplify the calculation process. As a result, these calculations were often overly conservative, leading to an increase in material volume or construction costs. Today, with the development of science and technology and advanced computational techniques, many calculation software programs based on numerical simulation using the finite element method have been developed, assisting in the analysis and calculation of complex problems in practical engineering. The studies by Zhang et al. [2], Osokin et al. [3], and Dang et al. [4] indicate that the internal force analysis results from numerical simulations (bending moments and shear forces) in diaphragm walls caused by deep excavations are consistent with the results obtained from field measurements.

The objective of this paper is to present a numerical simulation method for analyzing the behavior of reinforced concrete technical manholes on highways in Vietnam. The calculation using the approximate method (traditional method) is also presented to provide results for comparison with the numerical method proposed in the study. It is hoped that this paper will serve as a useful reference for researchers as well as design engineers in the calculation and design of reinforced concrete technical manholes on highways in Vietnam.

2. Structural Characteristics and Construction Method of Technical Manholes

A technical manhole is a junction point for technical pipelines, such as drainage pipes or pipes containing utility cables. Technical manholes are typically designed with sufficient size to allow easy access for people to enter for inspection, maintenance, and servicing of the pipes connected to the manhole. For drainage manholes, this also serves as a location for water collection, sedimentation, and the gathering of debris from wastewater to prevent blockages in the drainage pipes leading into the manhole. There are various types of technical manholes; based on their function, they can be classified into drainage manholes and manholes for utility conduit transfer. Based on the materials used, they can be categorized into reinforced concrete manholes, brick manholes, plastic manholes, composite manholes, and stainless steel manholes. In terms of construction methods, reinforced concrete manholes can be further divided into precast and cast-in-place manholes. Precast manholes usually have their own design and construction standards and are typically used for smaller-sized manholes. Cast-in-place reinforced concrete manholes are generally applied for larger-sized manholes. Figure 1 below shows the dimensions and structure of a cast-in-place reinforced concrete drainage technical manhole used at the parking area of the South Control Station, Hai Van 2 Tunnel [5]

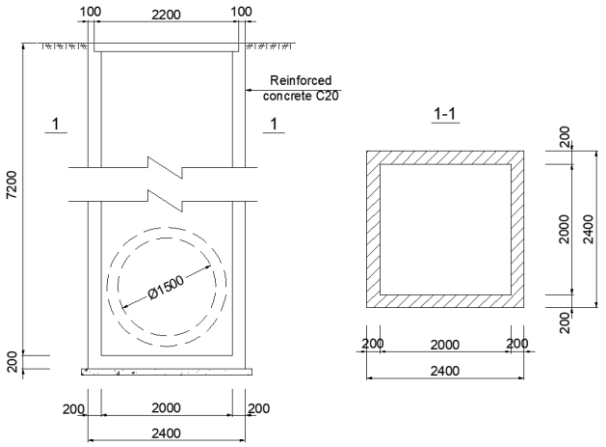

Figure 1. Structure and Dimensions of a Reinforced Concrete Technical Manhole.

The technical manhole above is constructed using the cast-in-place concrete method in an open excavation, specifically including the following steps:

- Excavate the foundation pit to the required depth of the manhole using open

excavation methods for the manhole construction;

- Install scaffolding, formwork, reinforcement steel, and cast the concrete in place for the technical manhole;
- Wait for the concrete to reach sufficient strength, then backfill the area around the manhole to the design elevation;
- Proceed with the construction of the pavement structure layer up to the top of the manhole and complete the finishing work.

3. Numerical Simulation Method

This section will present the numerical simulation method for analyzing the behavior of the reinforced concrete technical manhole shown in Figure 1 above using the Plaxis 3D software, 2023. Plaxis 3D is a 3D finite element program developed by Delft University of Technology and commercialized by PLAXIS Bv, Amsterdam, Netherlands. The Bridge Design Standard, designated TCVN 11823-2017 [6], is used to determine the calculation parameters for the structure and loads applied in this problem.

According to the Plaxis 3D reference manual [7], the influence zone of the surrounding backfill around the manhole is approximately three times the depth of the manhole. To increase the accuracy of the calculation results, the width of the surrounding backfill around the manhole is taken as 25.0 m. The good soil (bedrock, compacted sand, or clay in a firm state) located deep beneath the manhole undergoes very little deformation, so it is neglected in the calculation model and simulated as a rigid, deformation-free foundation. The natural soil layers above the good soil foundation and the backfill surrounding the manhole are modeled as linear elastic-perfectly plastic materials using the Mohr-Coulomb model (MC model), which is integrated into the Plaxis 3D software. According to the study by Ou [8], the MC model is a simple soil behavior model recommended for analyzing the behavior of structures placed in the ground, as it helps save memory and reduces the computational time of the numerical model. Other, more complex models, such as the Hardening Soil model (HS model) and the Hardening Soil model with Small Strain Stiffness (HSS model), are recommended for use only when precise analysis of soil settlement is required in regions with varying deformation levels . Since the reinforced concrete manhole undergoes very little deformation during loading, it can be modeled using plate elements and linear elastic materials.

The MC model is a basic material behavior model for soil, representing a first-order approximation of soil behavior. This model assumes that the stress-strain relationship of the soil is linear elastic-perfectly plastic, with the failure criterion being the Mohr-Coulomb failure criterion. The MC model includes five input parameters: the friction angle, cohesion, modulus of elasticity, Poisson's ratio, and the dilatancy angle.

For well-drained sandy soil layers, such as backfill and pavement structure layers, they will be modeled as drained materials along with effective strength parameters. In this case, the effective friction angle ($\boldsymbol{\phi'}$) is determined directly from drained laboratory tests; the effective cohesion ($\boldsymbol{c'}$) is assumed to be zero. However, to simplify the calculation process in the Plaxis software, a very small value of $\boldsymbol{c' = 0.5}$ kPa is used for the sandy soil layers. According to the recommendations of Plaxis 3D reference manual [7], the effective Poisson's ratio ($\boldsymbol{\nu'}$) for sandy soil layers is taken as 0.3. According to the research by Hwang et al. [9] and Bolton [10], the effective modulus of elasticity ($\boldsymbol{E'}$) and the effective dilatancy angle ($\boldsymbol{\psi'}$) for sandy soil layers are determined using the formulas below, where N is the blow count derived from the Standard Penetration Test (SPT).

$$\boldsymbol{E' = 2000N\ (kPa)} \quad (1)$$

When $\boldsymbol{\phi' \leq 30^o}$, then $\boldsymbol{\psi' = 0^o}$ (2)

When $\boldsymbol{\phi' > 30^o}$, then $\boldsymbol{\psi' = \phi' - 30^o}$ (3)

In contrast, for poorly drained clay layers, such as some natural clay layers above the good soil foundation, they will be modeled as

undrained materials with total strength parameters (Undrained C). In this case, the undrained friction angle is zero ($\boldsymbol{\phi_u = 0}$), the undrained cohesion is the undrained shear strength of the soil ($\boldsymbol{c_u = S_u}$), and the undrained modulus of elasticity ($\boldsymbol{E_u}$) and undrained Poisson's ratio ($\boldsymbol{\nu_u}$) are used for the analysis. The parameter $\boldsymbol{S_u}$ is determined directly from undrained shear tests. The Poisson's ratio $\boldsymbol{\nu_u}$ is taken as 0.495 (≈0.5) to simulate the incompressible behavior of water and to avoid numerical issues in the Plaxis software. According to the research by Khoiri and Ou [11], $\boldsymbol{E_u}$ can be determined using the following empirical equation:

$$\boldsymbol{E_u = 500 S_u} \quad (4)$$

Based on the analysis above, Tables 1 & 2 below presents the input parameters for the sandy and clayey soil layers in the calculation model.

According to the studies by Ou [8], Hwang et al. [9], and Khoiri & Ou [11], the walls of the technical manhole can be modeled using plate elements with a linear elastic material model. The input parameters for the plate elements include the modulus of elasticity ($\boldsymbol{E_c}$), Poisson's ratio ($\boldsymbol{\nu}$), plate thickness ($\boldsymbol{t}$), and the unit weight of the plate ($\boldsymbol{\gamma_c}$). According to ACI 318M-19 [12], the Poisson's ratio can be taken as 0.2, and the modulus of elasticity can be determined using the formula below, where $\boldsymbol{f'_c}$ is the specified compressive strength of concrete (MPa). Based on this, the input parameters for the manhole wall plates are provided in Table 3 below.

$$\boldsymbol{E_c = 4700\sqrt{f'_c}\ (MPa)} \quad (5)$$

The loads acting on the technical manhole include the self-weight of the manhole, the surrounding soil and water pressure, and the live load from vehicles running above. The construction process sequence includes the following stages: excavation of the foundation pit, construction of the manhole, backfilling, construction of the surrounding pavement structure, and finally, application of the live load from vehicles running above. However, it is evident that the most critical stage of the manhole's load-bearing is the final stage, which occurs after the live load from vehicles running above. Therefore, the simulation and calculation of the manhole only require four stages: 1) activation of all the natural soil layers, 2) activation of the backfill and the technical manhole, 3) excavation of all the soil inside the manhole (deactivating the soil layers inside the manhole), and 4) application of the live load from vehicles running above.

Table 1. Input parameters for the sandy soil layers in the calculation model.

Soil layers	Soil type	Thickness (m)	γ (kN/m³)	SPT-N	ϕ' (degree)	c' (kPa)	E' (kPa)	ν'	ψ' (degree)
Backfill soil	Sand	3.2	20.5	40	34	0.5	80000	0.3	4
Natural Soil 1	Sand	5.5	19.8	50	36	0.5	100000	0.3	6
Natural Soil 3	Sand	3.0	19.2	34	30	0.5	68000	0.3	0

Table 2. Input parameters for the clayey soil layers in the calculation model.

Soil layers	Soil type	Thickness (m)	γ (kN/m³)	ϕ_u (degree)	S_u (kPa)	E_u (kPa)	ν_u
Natural Soil 2	Clay	2.2	20.2	0	84	42000	0.495
Natural Soil 4	Clay	1.5	19.6	0	65	32500	0.495

Table 3. Input parameters for the manhole wall plates in the calculation model.

Parameters	Symbols	Values	Units
Specified compressive strength of concrete	f'_c	20	MPa
Modulus of elasticity	E_c	$2.1x10^7$	kN/m^2

Parameters	Symbols	Values	Units
Thickness	d	0.2	m
Unit weight	γ_c	24.5	kN/m^3
Poisson's ratio	ν	0.2	-

4. Results and discussion

In this section, the results of the numerical analysis for the reinforced concrete technical manhole, as modeled using Plaxis 3D, are presented and discussed. Figure 2 below shows the calculation model after excavating the soil inside the technical manhole, while Figure 3 illustrates the vertical deformation (displacement) of the backfill under the influence of the self-weight and uniformly distributed live load from the vehicle above. As shown, the maximum settlement of the backfill is found to be 2.1 mm.

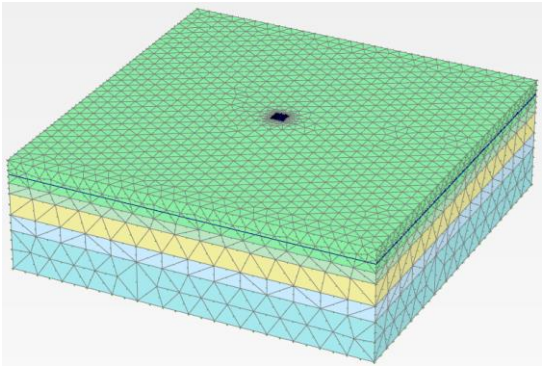

Figure 2. Calculation model after excavating the soil inside the technical manhole.

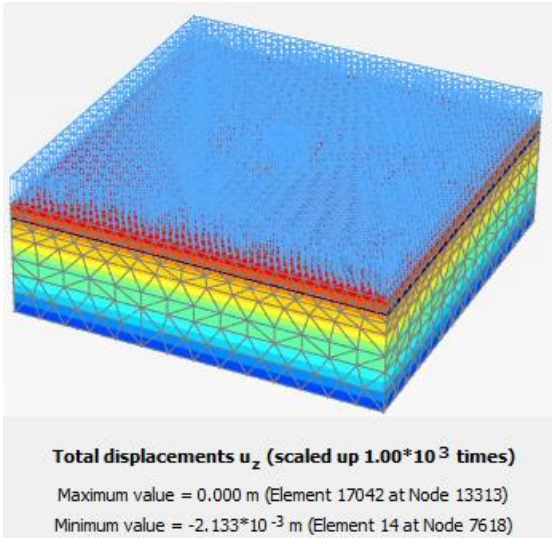

Figure 3. Vertical deformation of the backfill after applying the live load on top.

Figure 4 below illustrates the bending moment $\boldsymbol{M_{22}}$ (bending moment around axis 1 of the element) in the manhole structure, while Figure 5 shows the bending moment $\boldsymbol{M_{22}}$ in the manhole structure at a cross-section 5.5 meters from the top of the manhole. From Figures 4 and 5, it can be observed that the manhole structure experiences both positive and negative bending. Specifically, the manhole structure undergoes positive bending (tensile stress on the outer fibers) at the corners of the manhole and negative bending (tensile stress on the inner fibers) in the middle areas of the four side walls. The distribution of the bending moment $\boldsymbol{M_{22}}$ on the four side wall panels, which includes positive bending moments at the corners and negative bending moments at the mid-span, is reasonable because the side wall panels behave like three-edge fixed plates subjected to the distributed pressure of soil and water from the outside. In principle, the horizontal earth pressure increases with the depth of the manhole; therefore, the bending moment $\boldsymbol{M_{22}}$ will also increase with the depth of the manhole. However, as observed in Figure 4, the bending moment $\boldsymbol{M_{22}}$ reaches its maximum value at a depth of approximately two-thirds of the manhole's total depth measured from the top. This phenomenon is due to the three-dimensional effects (corner effects) of the manhole's base slab influencing the bending moment $\boldsymbol{M_{22}}$ in the four side walls of the manhole. Figure 5 shows that the maximum positive and negative bending moments of $\boldsymbol{M_{22}}$ are 13.3 kNm/m and 6.6 kNm/m, respectively. It can be observed that the positive bending moment is approximately twice as large as the negative bending moment. Therefore, the reinforcement for positive bending (horizontal outer-fiber reinforcement) should be greater than the

reinforcement for negative bending (horizontal inner-fiber reinforcement).

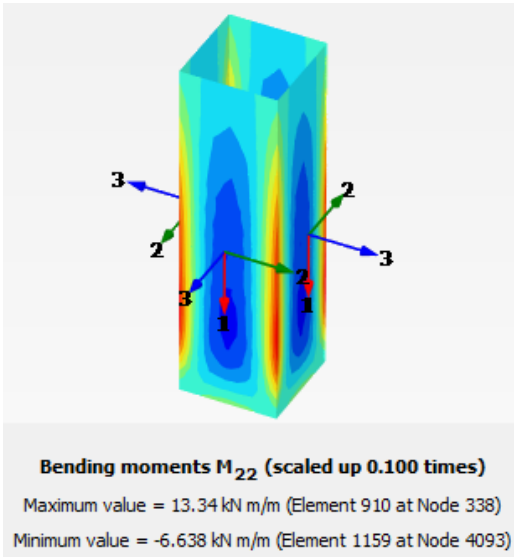

Figure 4. Bending Moment Diagram M_{22} in the Manhole Body.

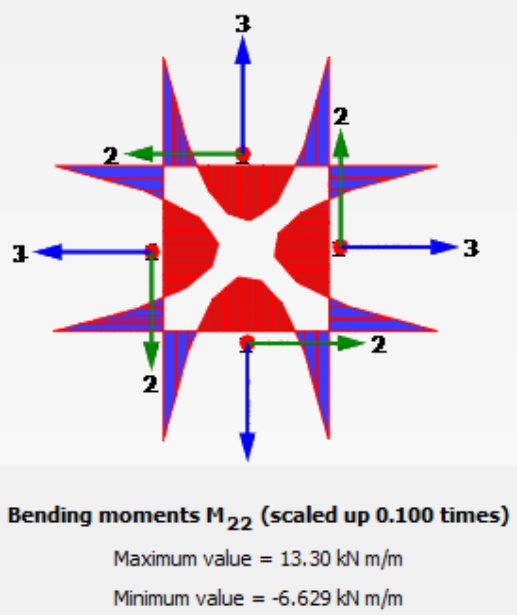

Figure 5. Bending Moment Diagram M_{22} in the Manhole Body at a Cross-Section 5.5m from the Top of the Manhole.

Figure 6 below illustrates the shear force $\boldsymbol{Q_{23}}$ in the manhole body, while Figure 7 shows the shear force $\boldsymbol{Q_{23}}$ in the manhole body at a cross-section 5.5 m from the top of the manhole. Similar to the bending moment, the shear force $\boldsymbol{Q_{23}}$ reaches its maximum value at a depth of approximately two-thirds of the manhole's total depth measured from the top. This is due to the three-dimensional effects (corner effects) of the manhole's base slab on the shear force $\boldsymbol{Q_{23}}$ at the four side walls of the manhole. Figure 7 shows that the maximum positive and negative shear forces of $\boldsymbol{Q_{23}}$ are 50.6 kN/m and 50.4 kN/m, respectively. It can be observed that the shear force $\boldsymbol{Q_{23}}$ reaches its maximum value at the corners and gradually decreases to zero at the mid-span. The distribution of the shear force $\boldsymbol{Q_{23}}$ on the four side wall panels is reasonable because these panels behave like three-edge clamped plates subjected to the distributed pressure of soil and water from the outside. Therefore, the placement of shear reinforcement (reinforcement perpendicular to the wall surface) is the same for both sides of each manhole wall panel.

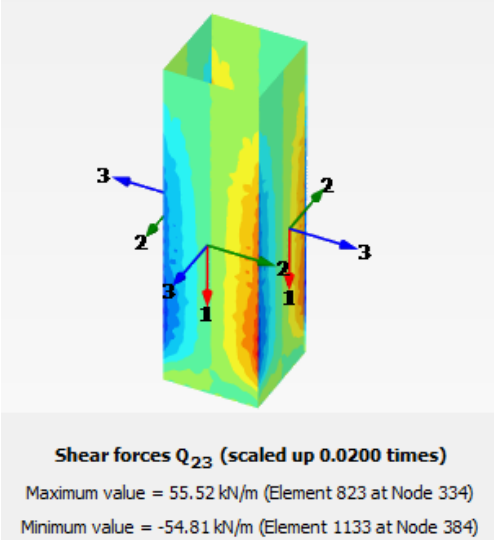

Figure 6. Shear Force Diagram Q_{23} in the Manhole Body.

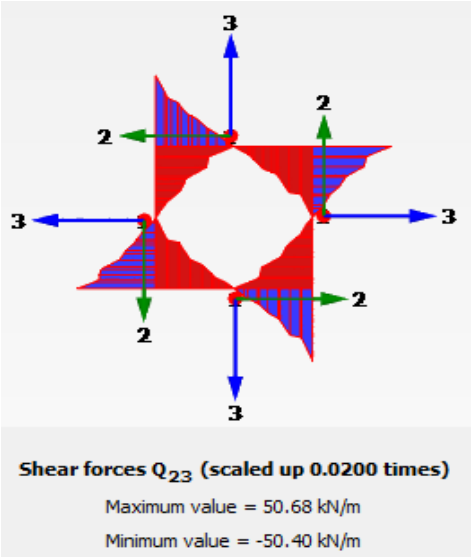

Figure 7. Shear Force Diagram Q_{23} in the Manhole Body at a Cross-Section 5.5 meters from the Top of the Manhole.

The bending moment $\boldsymbol{M_{22}}$ and shear force $\boldsymbol{Q_{23}}$ in the side walls of the technical manhole, at the cross-section 5.5 meters from the top of the manhole, can also be determined using the approximate method (traditional method). According to the approximate method, the first step is to determine the effective lateral pressure of soil, water, and the surcharge load on the side walls of the technical manhole using equation (6) below [13]. Where $\boldsymbol{K_o}$ is the coefficient of earth pressure at rest, determined using equation (7) below; $\boldsymbol{q}$ is the equivalent uniformly distributed load of the vehicle surcharge above; $\boldsymbol{\gamma_i}$ is the natural unit weight of the $\boldsymbol{i^{th}}$ soil layer above the groundwater table; hih_ihi is the thickness of the $\boldsymbol{i^{th}}$ soil layer above the groundwater table; $\boldsymbol{\gamma_i'}$ is the effective unit weight of the $\boldsymbol{i^{th}}$ soil layer below the groundwater table; $\boldsymbol{h_i'}$ is the thickness of the $\boldsymbol{i^{th}}$ soil layer below the groundwater table; and $\boldsymbol{\gamma_w}$ is the unit weight of water. The effective unit weight of the $\boldsymbol{i^{th}}$ soil layer below the groundwater table is determined using equation (8), where $\boldsymbol{\gamma_{isat}}$ is the saturated unit weight of the $\boldsymbol{i^{th}}$ soil layer below the groundwater table.

$$\boldsymbol{p = K_o(q + \sum \gamma_i h_i + \sum \gamma_i' h'_i) + \sum \gamma_w h'_i} \quad (6)$$

$$\boldsymbol{K_o = 1 - sin\phi'} \quad (7)$$

$$\boldsymbol{\gamma_i' = \gamma_{isat} - \gamma_w} \quad (8)$$

Next, assume that the effective lateral pressure of the soil, water, and surcharge load above is uniformly distributed over a strip of wall 1 meter wide and rigidly fixed at both ends. Suppose the wall operates in the linear elastic phase; in that case, $\boldsymbol{M_{22}}$ and $\boldsymbol{Q_{23}}$ are determined using the formula of a standard mechanical problem, as shown in Figure 8 below.

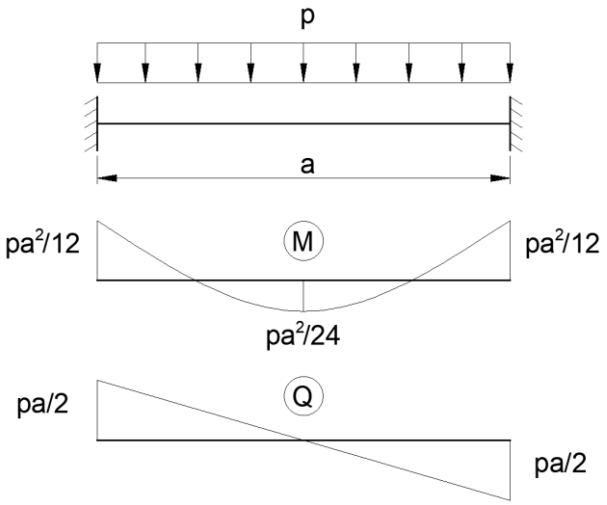

Figure 8. The bending moment and shear force diagrams for a strip of wall rigidly fixed at both ends under a uniformly distributed load.

Applying the above approximate assumptions, we find that the maximum negative and positive bending moments of $\boldsymbol{M_{22}}$ are 18.3 kNm/m and 9.2 kNm/m, respectively. The maximum positive and negative shear forces of $\boldsymbol{Q_{23}}$ are 55 kN/m and 55 kN/m. When compared with the results from the proposed numerical method above, we see that the results from the approximate method are overly conservative. The results for the bending moment and shear force calculated using the approximate method are about 1.4 times greater than the results from the numerical method. This could be because the approximate method does not consider the the three-dimensional effects of the base slab, as well as the surrounding wall sections of the strip wall under consideration.

From the above bending moment and shear force calculations, we can verify and/or design the reinforced concrete manhole structure. This includes selecting the manhole dimensions (thickness), the concrete grade, the reinforcement grade, as well as the quantity and arrangement of the reinforcement for the manhole body. For example, the calculation of the longitudinal tensile reinforcement due to the bending moment MMM according to the ACI 318M-19 standard [12] is performed following these steps:

Step 1: Determine the height of the equivalent rectangular compression stress block at the ultimate strength state (a) according to equation (9). In this equation, $\boldsymbol{\phi}$ is the bending strength reduction factor, bbb is the width of the considered slab, typically taken as 1 meter, and ddd is the distance from the centroid of the tensile reinforcement to the outermost concrete compression fiber.

$$\boldsymbol{\phi}[\mathbf{0.85}\boldsymbol{f_c'ba}(\boldsymbol{d}-\boldsymbol{a}/\mathbf{2})=\boldsymbol{M} \quad (9)$$

Step 2: Determine the area of the longitudinal tensile reinforcement for 1 meter of slab width ($\boldsymbol{A_s}$) with the assumption that the longitudinal tensile reinforcement yields plastically, according to equation (10). In this equation, $\boldsymbol{f_y}$ is the yield strength of the longitudinal tensile reinforcement.

$$\boldsymbol{A_s f_y}=\mathbf{0.85}\boldsymbol{f_c'ba} \quad (10)$$

Applying the above formulas, the design results show that the longitudinal tensile reinforcement for the positive and negative bending moments $\boldsymbol{M_{22}}$ are 5D8 @ 200 mm and 5D6 @ 200 mm, respectively, with the reinforcement made of CB400V steel according to TCVN 1651-2: 2018 [14].

5. Conclusion

This paper has presented a detailed numerical simulation method for analyzing the behavior of reinforced concrete technical manholes on highways in Vietnam, using Plaxis 3D software. The calculation results show the distribution of bending moments and shear forces within the manhole structure, which helps identify the factors affecting the design of the manhole structure. The finite element simulation allows for a more accurate assessment of complex factors such as surrounding soil pressure, traffic loads, and the interactions between the manhole's wall panels and base. It is found that the maximum positive and negative bending moments of $\boldsymbol{M_{22}}$ are 13.3 kNm/m and 6.6 kNm/m, respectively; the positive bending moment is approximately twice as large as the negative bending moment. The maximum positive and negative shear forces of $\boldsymbol{Q_{23}}$ are 50.6 kN/m and 50.4 kN/m, respectively. The calculation of bending moments and shear forces using the approximate method results in overly conservative outcomes; the results from the approximate method are about 1.4 times greater than those from the numerical method. The design results show that the longitudinal tensile reinforcement for the positive and negative bending moments $\boldsymbol{M_{22}}$ are 5D8 @ 200 mm and 5D6 @ 200 mm, respectively, with the reinforcement made of CB400V steel. The results emphasize the need for proper reinforcement selection and placement to ensure the manhole's load-bearing capacity, thereby reducing costs and optimizing the design's effectiveness. This simulation method can be a useful tool for supporting design engineers in the calculation and design of technical manholes, contributing to improving the quality of transportation infrastructure projects in Vietnam.

Declaration of competing interest and dedication to copyright

The authors declare the absence of any potential conflicts of interest from this study and affirm that the paper has not been previously published.

Data available

Data will or will not be provided upon request.

References

[1] Ministry of Science and Technology of Vietnam, Precast Thin-Walled Reinforced Concrete Manholes, TCVN 10333:2014, 2014.

[2] R. H. Zhang, A. T. C. Goh, and W. G. Zhang, "System reliability assessment on deep braced excavation adjacent to an existing upper slope in mountainous terrain: A case study," *SN Applied Sciences*, vol. 1, no. 1, Art. no. 876, 2019, doi: 10.1007/s42452-019-0938-x.

[3] A. Osokin, M. Paramonov, I. Dyakonov, and I. Bashmakov, "Determination of the bending moment in the diaphragm wall by inclinometric observations," *in Proc. E3S Web of Conferences*, vol. 371, Art. no. 02015, Feb. 2023, doi: 10.1051/e3sconf/202337102015.

[4] T. X. Dang, P. T. Nguyen, T. A. Nguyen, and H. V. V. Tran, "Optimization of barrette wall depths for

urban excavation stability using FEM and ANOVA testing," *Civil Engineering and Architecture*, vol. 12, no. 5, pp. 3530–3544, Sep. 2024, doi: 10.13189/cea.2024.120529.

[5] C. K. Le, *Detailed Design Documentation for Construction Drawings, Expansion of Hai Van Road Tunnel Project, Package for the Construction of the South Control Station of Hai Van Tunnel*, Hoang Long Construction Consulting Joint Stock Company, Vietnam, 2017.

[6] Ministry of Science and Technology, *"Vietnam, Bridge Design Standards,"* TCVN 11823-2017, 2017.

[7] *PLAXIS 3D Reference Manual*, Bentley Advancing Infrastructure, 2023.

[8] C. Y. Ou, *Deep Excavation: Theory and Practice. The Netherlands: Taylor & Francis*, 2006. [Online]. Available: https://www.routledge.com/Deep-Excavation-Theory-and-Practice/Ou/p/book/9780415403306

[9] R. N. Hwang, T. Y. Lee, C. R. Chou, and T. C. Su, "Evaluation of performance of diaphragm walls by wall deflection paths," *Journal of GeoEngineering*, vol. 7, no. 1, pp. 1–12, Apr. 2012, doi: 10.6310/jog.2012.7(1).1.

[10] M. D. Bolton, "The strength and dilatancy of sands," *Géotechnique*, vol. 36, no. 1, pp. 65–78, Mar. 1986, doi: 10.1680/geot.1986.36.1.65.

[11] M. Khoiri, C. Y. Ou, "Evaluation of deformation parameter for deep excavation in sand through case histories," *Computers and Geotechnics*, vol. 47, pp. 57–67, Jan. 2013, doi: 10.1016/j.compgeo.2012.06.009.

[12] *Building Code Requirements for Structural Concrete (ACI 318M-19)*, American Concrete Institute, Farmington Hills, MI, USA, 2019.

[13] B. M. Das, *Principles of Foundation Engineering*, 6th ed. USA: Thomson, 2007.

[14] Ministry of Science and Technology, *Steel for the Reinforcement of Concrete – Part 2: Ribbed Bars, TCVN 1651-2:2018*, Hanoi, Vietnam, 2018.